

MicroRNAs expressed by herpes simplex virus 1 during latent infection regulate viral mRNAs

Jennifer Lin Umbach¹, Martha F. Kramer², Igor Jurak², Heather W. Karnowski¹, Donald M. Coen² & Bryan R. Cullen¹

Herpesviruses are characterized by their ability to maintain life-long latent infections in their animal hosts. However, the mechanisms that allow establishment and maintenance of the latent state remain poorly understood. Herpes simplex virus 1 (HSV-1) establishes latency in neurons of sensory ganglia, where the only abundant viral gene product is a non-coding RNA, the latency associated transcript (*LAT*)^{1,2}. Here we show that *LAT* functions as a primary microRNA (miRNA) precursor that encodes four distinct miRNAs in HSV-1 infected cells. One of these miRNAs, miR-H2-3p, is transcribed in an antisense orientation to *ICP0*—a viral immediate-early transcriptional activator that is important for productive HSV-1 replication and thought to have a role in reactivation from latency³. We show that miR-H2-3p is able to reduce ICP0 protein expression, but does not significantly affect *ICP0* messenger RNA levels. We also identified a fifth HSV-1 miRNA in latently infected trigeminal ganglia, miR-H6, which derives from a previously unknown transcript distinct from *LAT*. miR-H6 shows extended seed complementarity to the mRNA encoding a second HSV-1 transcription factor, ICP4, and inhibits expression of ICP4, which is required for expression of most HSV-1 genes during productive infection⁴. These results may explain the reported ability of *LAT* to promote latency^{5–9}. Thus, HSV-1 expresses at least two primary miRNA precursors in latently infected neurons that may facilitate the establishment and maintenance of viral latency by post-transcriptionally regulating viral gene expression.

HSV-1 *LAT* is an ~8.3 kilobase (kb) capped, polyadenylated RNA (Fig. 1a)^{1,2} that is spliced to give a ~2.0 kb stable intron and a predicted ~6.3 kb unstable exonic RNA^{10,11}. Because *LAT* is not thought to encode a protein, we investigated whether the exonic regions of

LAT might function as a primary miRNA precursor¹². To identify HSV-1 *LAT*-derived miRNAs, we constructed a *LAT* expression plasmid, pcDNA3-*LAT*, in which a heterologous promoter drives transcription of an ~10.8 kb HSV-1 genomic fragment containing the entire 8.3 kb *LAT* (Fig. 1a). We transfected this plasmid into human 293T cells and isolated total RNA. Northern analysis showed high-level expression of the stable *LAT* intron (Fig. 1b).

Small RNAs derived from this sample were used to prepare complementary DNAs for 454 sequencing¹³. This resulted in 225,439 sequence reads (Supplementary Table 1), of which at least 144,955 represented cellular miRNAs (Supplementary Table 2A). We also recovered 651 HSV-1-derived miRNAs (Supplementary Tables 1 and 3). Six HSV-1 miRNA sequences were obtained, derived from four HSV-1 miRNA precursor hairpins (Fig. 2a). The two most common HSV-1 miRNAs were miR-H2-3p (265 reads) and miR-H4-3p (266 reads); these were derived from miRNA stem-loops that also gave rise to star strands miR-H2-5p (10 reads) and miR-H4-5p (61 reads) (Fig. 2a). We also detected miR-H3 (5 reads) and miR-H5 (40 reads). For each miRNA, HSV-1 *LAT* could be folded into the expected precursor stem-loop structure. Where both the miRNA and star strand were recovered, the characteristic ~2 nucleotide 3' overhangs were observed in the duplex intermediate (Fig. 2a).

These data show that *LAT* can be processed into miRNAs in culture but do not address expression *in vivo*. We therefore isolated small RNAs from trigeminal ganglia of mice latently infected with HSV-1 and performed deep sequencing of derived cDNAs. We obtained 254,651 sequence reads (Supplementary Table 1), of which at least 204,867 represent cellular miRNAs (Supplementary Table 2B). An extra 164 sequences represented HSV-1 miRNAs

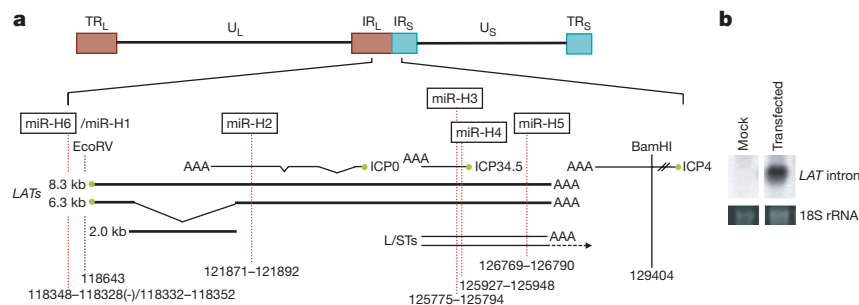


Figure 1 | Genomic location of HSV-1 miRNAs. **a**, Schematic of the HSV-1 genome expanded to show details of the *LAT* locus. Relative sizes, locations and orientations of other viral transcripts in this region are indicated. Sequence coordinates of viral miRNAs and restriction enzyme sites are given according to the HSV-1 strain 17 syn+ genome (NC_001806). All viral miRNAs are in the same orientation as *LAT* except for miR-H6. An EcoRV–BamHI fragment containing *LAT* was cloned into pcDNA3 to

generate pcDNA3-*LAT*. IR, internal repeat; TR, terminal repeat; U_L, unique long; U_S, unique short. **b**, Northern blot for the ~2.0 kb *LAT* intron, demonstrating *LAT* expression after transfection of pcDNA3-*LAT* into 293T cells. The lower bands show 18S ribosomal RNA which is a loading control. Small RNAs from this sample were used for cDNA preparation and 454 sequencing.

¹Department of Molecular Genetics and Microbiology and Center for Virology, Duke University Medical Center, Durham, North Carolina 27710, USA. ²Department of Biological Chemistry and Molecular Pharmacology, Harvard Medical School, Boston, Massachusetts 02115, USA.

(Supplementary Tables 1 and 4). miR-H2-3p (94 reads), miR-H3 (18 reads) and miR-H5 (1 read) represent *LAT*-derived miRNAs previously identified in *LAT*-expressing 293T cells (Fig. 2a). However, a fourth HSV-1 miRNA, miR-H6 (50 reads), derives from an RNA stem-loop transcribed from the opposite strand of the HSV-1 genome within the *LAT* promoter (Fig. 1a). This sequence was not present in pcDNA3-LAT and therefore could not be detected in transfected 293T cells. Of the total of 171 HSV-1 short RNAs detected in trigeminal ganglia, 27 were obtained only once. Of these, 20 represent truncations or point mutants of miR-H2 to miR-H6, whereas 7 seem to represent random HSV-1 RNA breakdown products (Supplementary Table 1 and data not shown).

The identification of miR-H6 is notable for two reasons. First, miR-H6 must derive from a second HSV-1 primary miRNA precursor, distinct from *LAT*, expressed in latently-infected neurons. Although a transcript in the antisense orientation to the *LAT* promoter has been described previously¹⁴, the reported ends of this transcript exclude miR-H6. The lack of previous reports describing this primary miRNA precursor may reflect the fact that it must be cleaved to generate miR-H6 and hence is probably unstable. Second, the stem-loop that gives rise to miR-H6 lies antisense to a stem-loop transcribed from the opposite DNA strand that gives rise to a previously described HSV-1 miRNA, miR-H1 (Fig. 2a). miR-H1 is expressed late in productive replication¹⁵ and shows extensive sequence complementarity with miR-H6 (Fig. 2b). The unusual phenomenon of distinct miRNAs derived by bidirectional transcription of a single genomic locus was recently also described in mouse cytomegalovirus¹⁶.

To ascertain whether any of these HSV-1 miRNAs are expressed during productive HSV-1 infection—where *LAT* is expressed late in infection¹¹—we performed stem-loop reverse transcription followed by quantitative polymerase chain reaction (qRT-PCR) for miR-H2-3p to miR-H6 using RNA from HSV-1-infected Vero cells. The cellular miRNA let-7a was used as an internal control for RNA recovery. All five HSV-1 miRNAs were detected in infected Vero cells using qRT-PCR (Fig. 2c and Supplementary Table 5A) and/or northern analysis (Supplementary Fig. 2d). The ‘non-*LAT*’ HSV-1 miRNA miR-H6 was detected at $10^{5.0}$ molecules per ng of isolated short (<200 nucleotides) RNA, whereas the four *LAT*-derived miRNAs were detected at between $10^{2.7}$ (miR-H3) and $10^{4.1}$ (miR-H2-3p)

molecules per ng (Fig. 2c and Supplementary Table 5A). These data confirm that all five novel HSV-1 miRNAs are expressed in productively infected cells.

qRT-PCR analysis of pcDNA3-LAT-transfected 293T cells (Fig. 2c) also detected all four *LAT*-derived miRNAs, but as expected did not detect miR-H6, which is not encoded by this vector. Analysis of short RNAs derived from mouse trigeminal ganglia demonstrated the expression of all four *LAT*-derived HSV-1 miRNAs, as well as miR-H6 (Fig. 2c and Supplementary Table 5A). There is a relatively poor correlation between the levels of expression of each HSV-1 miRNA, as extrapolated from deep sequencing, when compared to the qRT-PCR analysis. This presumably reflects differences in the efficiency of cDNA synthesis.

The qRT-PCR analysis presented in Fig. 2c and Supplementary Table 5A allows us to estimate roughly how many copies of each HSV-1 miRNA are present in productively infected Vero cells versus latently infected neurons. During productive infection, miR-H1 and miR-H6 are expressed at $\sim 1,200$ and ~ 300 copies per Vero cell. In contrast, the *LAT*-derived HSV-1 miRNAs miR-H2-3p to miR-H5 are all present at <40 copies per cell (Supplementary Table 6A). These latter levels may be too low to exert a significant phenotypic effect. In latently infected trigeminal ganglia, our estimate derives from a previous report that mice latently infected with the HSV-1 strain KOS contain ~ 500 *LAT*-expressing neurons per trigeminal ganglion¹⁷. On the basis of this report, we estimate $\sim 6.3 \times 10^4$ copies per *LAT*⁺ neuron for miR-H2-3p, $\sim 4 \times 10^4$ copies per *LAT*⁺ neuron for miR-H6 and $\sim 8 \times 10^5$ copies per *LAT*⁺ neuron for miR-H4-3p. We also detected substantial amounts of miR-H4-5p ($\sim 3.2 \times 10^4$ copies per *LAT*⁺ neuron), thus suggesting that the star strand of miR-H4 might also be a functional miRNA (Fig. 2c and Supplementary Table 6C). Even if our estimate of the number of latently HSV-1 infected neurons per trigeminal ganglia is low by an order of magnitude¹⁸, the level of HSV-1 miRNAs per neuron would still be within the range of cellular miRNAs that is biologically active¹².

Although we were able to detect several different HSV-1 miRNAs in both *LAT*-expressing 293T cells and infected Vero cells, we did not detect the previously described miR-LAT¹⁹ using a range of techniques (Supplementary Figs 1 and 2). The report describing miR-LAT was recently retracted.

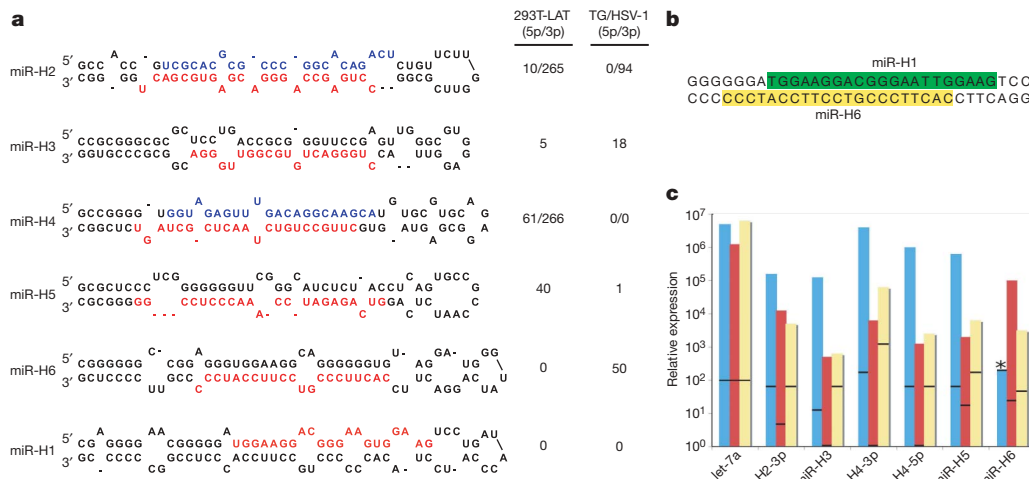


Figure 2 | HSV-1 pre-miRNAs. **a**, Predicted secondary structures of HSV-1 miRNA precursors, demonstrating the characteristic stem-loops. Mature miRNAs are indicated in red and, where observed, star strands are indicated in blue. The numbers of reads of each recovered mature miRNA sequence are indicated for *LAT*-transfected 293T cells (293T-LAT) and for trigeminal ganglia (TG) of mice infected with HSV-1. Where the star strand was also obtained, these are given as 5p/3p. miR-H1 and miR-H6 were not recovered from transfected 293T cells because pcDNA3-LAT lacks these sequences. **b**, HSV-1 genomic sequence showing the antisense orientation and overlap

of mature miR-H6, and the predicted sequence of miR-H1 (ref. 15). **c**, qRT-PCR analysis verifying the existence and relative expression of HSV-1 miRNAs in 293T cells transfected with pcDNA3-LAT (blue), Vero cells infected with HSV-1 (red), or mouse trigeminal ganglia latently infected with HSV-1 (yellow). miRNA abundances are shown as copies per ng of short-enriched RNAs (<200 nucleotides). Horizontal lines indicate background levels for each miRNA assayed. Asterisk, not detected. See Supplementary Table 5 for relevant controls.

Mapping of the six HSV-1 miRNAs onto the HSV-1 genome demonstrates that miR-H2 is antisense to the *ICP0* transcript, whereas both miR-H3 and miR-H4 are antisense to *ICP34.5* (Fig. 1a). *ICP0* is an HSV-1 transcriptional activator, expressed as an immediate-early gene, which promotes viral replication and may facilitate reactivation from latency^{3,20,21}. To examine whether miR-H2-3p could affect ICP0 protein or mRNA expression, we transfected 293T cells with either a wild-type ICP0 expression plasmid or a derivative containing three point mutations within the predicted miR-H2-3p seed region (Fig. 3a). These plasmids were co-transfected with plasmids designed to express a short hairpin RNA (shRNA) that mimics the predicted *miR-H2* pre-miRNA (Fig. 2a and Supplementary Fig. 3) or a mutated version of the *miR-H2* pre-miRNA (miR-H2-3M) that bears three mutations in the miR-H2-3p seed region that restore complementarity to the ICP0 mutant (Fig. 3a). As shown in Fig. 3b, the wild-type *miR-H2* pre-miRNA inhibited expression of wild-type, but not mutant, ICP0 protein. Conversely, expression of the mutant ICP0 protein was reduced on co-expression of the mutant *miR-H2-3M* pre-miRNA but was not affected by wild-type *miR-H2*. Although these data demonstrate that miR-H2-3p is acting through the expected target site to inhibit ICP0 protein expression, this inhibition did not correlate with a reduction in the level of *ICP0* mRNA (Fig. 3c). Similar data, obtained using short interfering RNA (siRNA) duplexes designed to mimic the miR-H2 or miR-H2-3M miRNA duplex intermediate, and using RNase protection to measure *ICP0* mRNA expression, are presented in Supplementary Fig. 3. Together, these data show that, despite the perfect complementarity of miR-H2-3p to *ICP0* mRNA, inhibition of ICP0 protein expression by this viral miRNA occurs primarily at the translational level¹². These data are consistent with earlier reports suggesting that *LAT* reduces ICP0 protein, but not mRNA, levels in infected cells^{22,23}.

Analysis of other HSV-1 genes showed sequence similarity between miR-H6, including an extended miRNA seed region¹², and the mRNA encoding ICP4, a transcription factor required for expression of most HSV-1 genes during productive infection (Fig. 4a)⁴. Co-transfection of an ICP4 expression plasmid with a synthetic form of the predicted miR-H6 duplex intermediate showed strong downregulation of ICP4 protein expression (Fig. 4b), whereas

an ICP4 expression construct with three mutations in the seed region of the predicted miR-H6 target site remained unaffected. Analysis of wild-type *ICP4* mRNA expression levels showed that miR-H6 co-expression had little or no inhibitory effect (Fig. 4c).

Here we report the identification of five HSV-1 miRNAs, three of which were previously computationally predicted^{15,24}. Four of these viral miRNAs derive from the second exon of the spliced ~6.3 kb *LAT* (Fig. 1a) and may provide both a rationale for the existence of spliced *LAT* and explain its characteristic instability^{1,11}, that is, *LAT* is probably degraded in the nucleus due to Drosha cleavage¹². In addition to the four *LAT*-derived HSV-1 miRNAs, we also identified a fifth miRNA, miR-H6, derived from an at present unknown primary miRNA precursor that lies antisense to the *LAT* promoter and which must also be expressed in latently infected neurons (Fig. 1a). Of interest, miR-H6 lies antisense to a known late HSV-1 miRNA, miR-H1 (ref. 15).

Three of the latently expressed HSV-1 miRNAs are transcribed antisense to HSV-1 mRNAs—*ICP0* mRNA in the case of miR-H2-3p and *ICP34.5* mRNA in the case of both miR-H3 and miR-H4-3p (Fig. 1a)—and we have demonstrated that miR-H2-3p is able to inhibit ICP0 protein expression (Fig. 3b). Because ICP0 is a key immediate-early HSV-1 transcriptional activator that may promote entry into the productive replication cycle^{3,20,21}, inhibition of ICP0 expression by miR-H2-3p may increase the likelihood that neurons enter and maintain latency. It has been previously proposed that *LAT* inhibits ICP0 expression post-transcriptionally in neurons^{2,10,23} and the existence of miR-H2-3p could explain this phenomenon. We also observed that miR-H6 shows partial complementarity to *ICP4* mRNA, including an extended miRNA seed region¹², and can reduce ICP4 protein expression (Fig. 4). Similar to ICP0, ICP4 can promote exit from latency²¹, and inhibition of ICP4 expression may therefore enhance the robustness of the latent state.

Although we have not directly examined the effect of miR-H3 and miR-H4-3p on *ICP34.5* expression, it seems probable that these viral miRNAs are also acting as inhibitors of viral gene expression. Data favouring this hypothesis come from analysis of the long/short junction spanning transcripts (L/STs) that overlap the 3' end of *LAT* (Fig. 1a). L/STs are expressed by HSV-1 mutants lacking ICP4 (ref. 25). Notably, the L/STs, which have the potential to give rise to miR-H3 and miR-H4-3p (Fig. 1a), are known to inhibit *ICP34.5* expression by an 'antisense' mechanism^{26,27}, and these viral miRNAs are

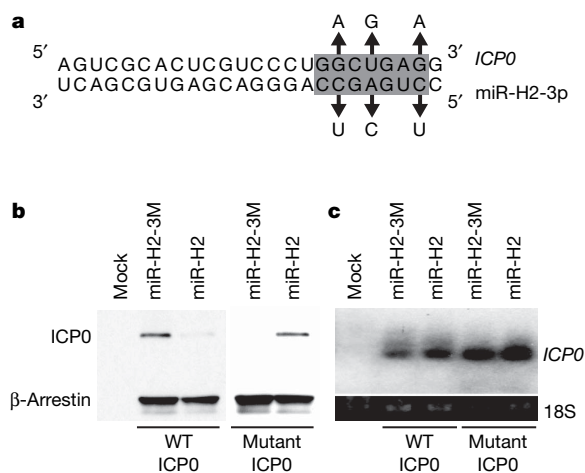


Figure 3 | Downregulation of ICP0 protein expression by HSV-1 miR-H2-3p. **a**, Sequence of miR-H2-3p bound to *ICP0* mRNA. The miRNA seed region is indicated in grey; arrows indicate complementary nucleotide changes introduced into the mutant ICP0 expression plasmid and miR-H2-3p-3M expression construct. **b**, Western blot analysis of ICP0 protein expression. 293T cells were transfected with a β -arrestin expression plasmid and either a wild-type (WT) or a mutant ICP0 expression construct. Plasmids expressing either miR-H2-3p or miR-H2-3p-3M were co-transfected. **c**, Northern analysis of the samples shown in **b**. 18S rRNA was used as a loading control.

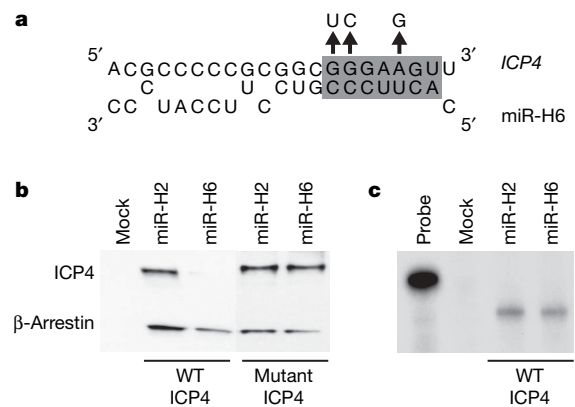


Figure 4 | Downregulation of ICP4 protein expression by HSV-1 miR-H6. **a**, Sequence complementarity of miR-H6 to nucleotides 127,298 to 127,319 of the *ICP4* mRNA. The grey box indicates the miRNA seed region; arrows indicate nucleotide changes present in the ICP4 mutant. **b**, Western blot analysis of ICP4 protein expression. 293T cells were co-transfected with a synthetic miR-H6 duplex intermediate and plasmids expressing either wild-type ICP4 or the ICP4 mutant. An miR-H2 duplex intermediate served as a negative control as *ICP4* mRNA has no predicted target sites for miR-H2-3p. **c**, RNase protection analysis of *ICP4* mRNA levels in the wild-type ICP4 samples shown in **b**.

presumably responsible for this effect. Our observation that HSV-1 miRNAs are capable of downregulating key viral immediate early proteins is consistent with the recent proposal—based primarily on computational data—that herpesviruses in general may use viral miRNAs “as part of their strategy to enter and maintain latency”²⁸.

METHODS SUMMARY

pcDNA3-LAT expresses a ~10.8 kb EcoRV to BamHI fragment, derived from the KOS strain of HSV-1, which extends 134 bp 5', and ~2.3 kb 3', to LAT. Small RNAs were prepared using standard techniques from 293T cells transfected with pcDNA3-LAT or from the dissected trigeminal ganglia of mice latently infected with HSV-1 strain KOS 30 days previously. cDNAs were prepared and subjected to 454 sequencing¹³. Vero or SY5Y cells were infected with HSV-1 strain KOS or strain 17syn+ at 10 plaque-forming units per cell, and RNA was collected for qRT-PCR analysis 14 to 18 h after infection. Northern and western blot analyses were performed using standard methods. Stem-loop qRT-PCR methods are described in Supplementary Information.

Full Methods and any associated references are available in the online version of the paper at www.nature.com/nature.

Received 29 April; accepted 16 May 2008.

Published online 2 July 2008.

- Bloom, D. C. HSV LAT and neuronal survival. *Int. Rev. Immunol.* **23**, 187–198 (2004).
- Stevens, J. G., Wagner, E. K., Devi-Rao, G. B., Cook, M. L. & Feldman, L. T. RNA complementary to a herpesvirus alpha gene mRNA is prominent in latently infected neurons. *Science* **235**, 1056–1059 (1987).
- Everett, R. D. ICP0, a regulator of herpes simplex virus during lytic and latent infection. *Bioessays* **22**, 761–770 (2000).
- Preston, C. M. Control of herpes simplex virus type 1 mRNA synthesis in cells infected with wild-type virus or the temperature-sensitive mutant *tsK*. *J. Virol.* **29**, 275–284 (1979).
- Chen, S. H., Kramer, M. F., Schaffer, P. A. & Coen, D. M. A viral function represses accumulation of transcripts from productive-cycle genes in mouse ganglia latently infected with herpes simplex virus. *J. Virol.* **71**, 5878–5884 (1997).
- Garber, D. A., Schaffer, P. A. & Knipe, D. M. A LAT-associated function reduces productive-cycle gene expression during acute infection of murine sensory neurons with herpes simplex virus type 1. *J. Virol.* **71**, 5885–5893 (1997).
- Thompson, R. L. & Sawtell, N. M. Herpes simplex virus type 1 latency-associated transcript gene promotes neuronal survival. *J. Virol.* **75**, 6660–6675 (2001).
- Thompson, R. L. & Sawtell, N. M. The herpes simplex virus type 1 latency-associated transcript gene regulates the establishment of latency. *J. Virol.* **71**, 5432–5440 (1997).
- Sawtell, N. M. & Thompson, R. L. Herpes simplex virus type 1 latency-associated transcription unit promotes anatomical site-dependent establishment and reactivation from latency. *J. Virol.* **66**, 2157–2169 (1992).
- Farrell, M. J., Dobson, A. T. & Feldman, L. T. Herpes simplex virus latency-associated transcript is a stable intron. *Proc. Natl Acad. Sci. USA* **88**, 790–794 (1991).
- Kang, W. *et al.* Characterization of a spliced exon product of herpes simplex type-1 latency-associated transcript in productively infected cells. *Virology* **356**, 106–114 (2006).
- Bartel, D. P. MicroRNAs: genomics, biogenesis, mechanism, and function. *Cell* **116**, 281–297 (2004).
- Hafner, M. *et al.* Identification of microRNAs and other small regulatory RNAs using cDNA library sequencing. *Methods* **44**, 3–12 (2008).
- Perng, G. C. *et al.* A novel herpes simplex virus type 1 transcript (AL-RNA) antisense to the 5' end of the latency-associated transcript produces a protein in infected rabbits. *J. Virol.* **76**, 8003–8010 (2002).
- Cui, C. *et al.* Prediction and identification of herpes simplex virus 1-encoded microRNAs. *J. Virol.* **80**, 5499–5508 (2006).
- Dölken, L. *et al.* Mouse cytomegalovirus microRNAs dominate the cellular small RNA profile during lytic infection and show features of posttranscriptional regulation. *J. Virol.* **81**, 13771–13782 (2007).
- Feldman, L. T. *et al.* Spontaneous molecular reactivation of herpes simplex virus type 1 latency in mice. *Proc. Natl Acad. Sci. USA* **99**, 978–983 (2002).
- Sawtell, N. M. Comprehensive quantification of herpes simplex virus latency at the single-cell level. *J. Virol.* **71**, 5423–5431 (1997).
- Gupta, A., Gartner, J. J., Sethupathy, P., Hatzigeorgiou, A. G. & Fraser, N. W. Anti-apoptotic function of a microRNA encoded by the HSV-1 latency-associated transcript. *Nature* **442**, 82–85 (2006).
- Cai, W. *et al.* The herpes simplex virus type 1 regulatory protein ICP0 enhances virus replication during acute infection and reactivation from latency. *J. Virol.* **67**, 7501–7512 (1993).
- Halford, W. P., Kemp, C. D., Isler, J. A., Davido, D. J. & Schaffer, P. A. ICP0, ICP4, or VP16 expressed from adenovirus vectors induces reactivation of latent herpes simplex virus type 1 in primary cultures of latently infected trigeminal ganglion cells. *J. Virol.* **75**, 6143–6153 (2001).
- Chen, S. H. *et al.* Neither LAT nor open reading frame P mutations increase expression of spliced or intron-containing ICP0 transcripts in mouse ganglia latently infected with herpes simplex virus. *J. Virol.* **76**, 4764–4772 (2002).
- Thompson, R. L., Shieh, M. T. & Sawtell, N. M. Analysis of herpes simplex virus ICP0 promoter function in sensory neurons during acute infection, establishment of latency, and reactivation *in vivo*. *J. Virol.* **77**, 12319–12330 (2003).
- Pfeffer, S. *et al.* Identification of virus-encoded microRNAs. *Science* **304**, 734–736 (2004).
- Yeh, L. & Schaffer, P. A. A novel class of transcripts expressed with late kinetics in the absence of ICP4 spans the junction between the long and short segments of the herpes simplex virus type 1 genome. *J. Virol.* **67**, 7373–7382 (1993).
- Randall, G. & Roizman, B. Transcription of the derepressed open reading frame P of herpes simplex virus 1 precludes the expression of the antisense $\gamma_134.5$ gene and may account for the attenuation of the mutant virus. *J. Virol.* **71**, 7750–7757 (1997).
- Lee, L. Y. & Schaffer, P. A. A virus with a mutation in the ICP4-binding site in the L/ST promoter of herpes simplex virus type 1, but not a virus with a mutation in open reading frame P, exhibits cell-type-specific expression of $\gamma_134.5$ transcripts and latency-associated transcripts. *J. Virol.* **72**, 4250–4264 (1998).
- Murphy, E., Vanicek, J., Robins, H., Shenk, T. & Levine, A. J. Suppression of immediate-early viral gene expression by herpesvirus-coded microRNAs: implications for latency. *Proc. Natl Acad. Sci. USA* **105**, 5453–5458 (2008).

Supplementary Information is linked to the online version of the paper at www.nature.com/nature.

Acknowledgements We thank R. Sandri-Goldin for reagents used in this research and S. Boissel for contributions to PCR primer design. This work was supported by National Institutes of Health grants to B.R.C. and D.M.C.

Author Information Reprints and permissions information is available at www.nature.com/reprints. Correspondence and requests for materials should be addressed to B.R.C. (culle002@mc.duke.edu).

METHODS

Cells, viruses and RNA. 293T and Vero cells were maintained in DMEM supplemented with 10% fetal bovine serum and 5% newborn bovine serum, respectively. SY5Y cells were maintained in RPMI supplemented with 10% fetal bovine serum. Total RNA was extracted using Trizol (Invitrogen) or mirVana miRNA Isolation Kit (Ambion). HSV-1 strain KOS was propagated and assayed as described²⁹.

Plasmid constructs, siRNAs and transfections. pcDNA3-LAT was derived from an EcoRV–BamHI digest of pSG28 (ref. 30), which released adjacent EcoRI–BamHI and BamHI–BamHI fragments. These fragments contain the entire ~8.3 kb LAT, as well as an additional ~130 bp 5' of the cap site, and ~2.3 kb 3' of the polyadenylation signal. These fragments were ligated into pcDNA3.1(–)/Zeo (Invitrogen) and screened to verify orientation. Transfection of pcDNA3-LAT into 293T cells was performed using FuGene (Roche).

The ICP0 and ICP4 expression constructs pRS-1 and pSG28K/B, respectively, have been described previously³¹. pRS-1 contains the entire *ICP0* gene, whereas pSG28K/B contains the entire *ICP4* gene, both including the cognate promoter and poly(A) site, inserted into pUC18.

The ICP0-3M mutant was generated by PCR using two primer pairs. The 5' half of the mutant was generated using primers 5'-TCTGTTCTTGGTTCGCGCTGCGTCAGGGACGAGTGCGACT-3' and 5'-CGCTCGAGAACAGAGACCCCATAGTGATCA-3'. The 3' half was generated using primers 5'-AGTCGCACTCGTCCCTGACGCAAGCCGGAACCAAGAACA-3' and 5'-CGGAATTCTGAGTCGGAGGGGGTTCGTC-3'. The two PCR products were then woven together using recombinant PCR. The product was then digested with MluI/BclI and ligated into a similarly digested pRS-1 vector grown in SCS110 dam[–]/dcm[–] bacteria (Stratagene).

The ICP4 mutant was also generated by PCR. pUC18 was modified by inserting annealed oligonucleotides containing unique BsaAI/XhoI/DraIII sites into the vector HindIII/EcoRI sites. A fragment extending from the ICP4 BsaAI site to the miR-H6 binding site was then generated by PCR, which also introduced an XhoI site into the miRNA seed, using primers 5'-CCGCTGCGGC CCGTGTACGTGGCGCTGGGGCGCGAGGCGGTGCGCGCCGGCCCGCCGCGC-3' and 5'-CGTCCAGGCGCCTTCCAGTCCACAACCTCGAGCCGC GGGGGCGTGGCCAAGCCCGCT-3'. This fragment was then digested with BsaAI/XhoI and ligated into the modified pUC18. A second PCR fragment from the miR-H6 binding site to the ICP4 DraIII site was then generated using primers 5'-AGGCGGGCTTGCCACGCCCCCGCGGCTC GAGGTGTGGACTGGGAAGGCGCCTGGGACG-3' and 5'-CGGCGCGCC AGGCGGGCGCCGAGGCCAGACCACAGGTGGCGCACCCGGACGTG GGG-3'. Like the first PCR product, this fragment also introduced an XhoI site into the miR-H6 seed. The fragment was digested with XhoI/DraIII and ligated into the pUC18 vector containing the mutant BsaAI/XhoI ICP4 fragment. The entire mutant ICP4 fragment was then transferred into pSG28K/B to generate the ICP4 mutant.

shmiR-H2-3p expression constructs were generated by annealing together oligonucleotides 5'-GATCCCCGTCGACGCGCCCTGGCATAGACTTGA CCTGAGCCAGGGACGAGTGCAGCTTTTT-3' and 5'-AGCTAAAAAGTCCG ACTCGTCCCTGGCTCAGGTCCAAGTCTATGCCAGGGCGGTGCGACGG G-3' and ligating them into BglII/HindIII-digested pSUPER³². shmiR-H2-3p-3M was constructed similarly using oligonucleotides 5'-GATCCCCGT CGCAGCGCCCTGACATAAACTTGGACTTGCCTCAGGGACGAGTGCAGG CTTTTT-3' and 5'-AGCTAAAAAGTCCGACTCGTCCCTGACGCAAGTCC AAGTTTATGTCAGGGCGGTGCGACGGG-3'.

The ICP0 riboprobe used for northern blot analysis was generated by *in vitro* transcription of linearized pcDNA3.1(–)/Zeo vector containing a 431 bp BamHI-XhoI *ICP0* gene fragment. The ICP0 riboprobe used for RPA was generated by *in vitro* transcription of a linearized pcDNA3 vector containing a 284 bp fragment of ICP0 that overlaps the miR-H2 binding site. The ICP4 riboprobe was generated by *in vitro* transcription of a linearized pcDNA3 vector containing a 194 bp NotI/BamHI fragment of ICP4. The HA-tagged β -arrestin expression plasmid has been described previously³³.

siRNA duplexes designed to mimic the miR-H2 and miR-H6 miRNA duplex intermediates, and a mutant form with 3 mutations (3M) in the miR-H2-3p seed region, were obtained from IDT. miR-H2-3p duplex 5' arm 5'-UCGCACUCGUCCUGGUCAGACU-3'; miR-H2-3p duplex 3' arm 5'-CCUGAGCCAGGGACGAGUGCGACU-3'; miR-H2-3p-3M duplex 5' arm 5'-UCGCACUCGUCCUGGUCAGCAACU-3'; miR-H2-3p-3M duplex 3' arm 5'-CUUGCGUCAGGGACGAGUGCGACU-3'; miR-H6 duplex 5' arm 5'-GAUGGAAGGACGGGAAGUAUA-3'; miR-H6 duplex 3' arm 5'-CACUCCCGUCCUCCAUCCC-3'. All plasmid DNA and siRNA cotransfections were performed in 293T cells using Lipofectamine 2000 (Invitrogen).

Briefly, 293T cells were plated in 24-well plates to be 80%–90% confluent on the next day. Cells were co-transfected with either 60–80 ng of an ICP0 expression plasmid or 40–60 ng of an ICP4 expression plasmid, 30 ng of β -arrestin-HA, and 10 pmol of the appropriate siRNA duplex or 100 ng of the relevant shRNA expression vector. One microlitre of Lipofectamine 2000 was used per well per transfection. Samples were transfected in duplicate and collected simultaneously ~24 h after transfection. One sample was collected for western blot and the other for RNA analysis.

454 sequencing. Sample preparation for 454 sequencing was conducted as described³⁴, up to and including the RT-PCR step. After that point, the protocol as outlined by the Hannon laboratory on the 454 website (<http://www.454.com>) was followed. Initially, 750 μ g of total RNA from pcDNA3-LAT transfected 293T cells, and 60 μ g of total RNA from latently-infected mouse trigeminal ganglia, was used. Data analysis was performed using Microsoft Excel and BLAST. Briefly, raw data from 454 was indexed and binned to give a list and count of all unique sequences. The 5' and 3' linker sequences were parsed out and final sequences 18–24 nucleotides in length occurring twice or more were analysed by BLAST (v2.2.17) against either the mature human or the mouse miRNA databases downloaded from miRBASE (release 9.2). Sequences identified as host miRNAs were annotated, indexed and removed from subsequent analysis. Remaining sequences were then analysed against the HSV-1 genome (NC_001806) to identify potential HSV-1 miRNAs. Candidate HSV-1 miRNA sequences and flanking regions were analysed by mfold to predict the secondary structures at each locus.

Northern blots, RPA and splint-ligation assay. For the ICP0 northern blot, 5 μ g of total RNA was separated on a 0.6% agarose gel, transferred onto nitrocellulose, ultraviolet-irradiated and hybridized with the ICP0 riboprobe at 68 °C and washed at 85 °C, according to standard protocols. Bands were visualized by autoradiography. The LAT intron was detected by northern blot using an oligonucleotide probe, as described³⁵. *ICP4* and *ICP0* mRNA levels were measured using an Ambion HybSpeed RPA kit with 5 μ g of total RNA. Splint-ligation assays (USB) were performed using 12 μ g of total RNA per sample.

Western blots. Samples were collected and run on 4–20% Tris-HCl gels (Bio-Rad), which were then transferred onto nitrocellulose and probed with mouse monoclonal antibodies specific for ICP0 or ICP4 (Virusys), or anti-HA monoclonal antibody (Covance). Blots were then incubated with an anti-mouse secondary antibody (GE Healthcare) and bands were visualized with Lumi-Light Western Blotting Substrate (Roche).

Latent HSV infection in mice. Procedures involving mice were approved by the Harvard Medical School Institutional Animal Care and Use Committee in accordance with federal guidelines. Male CD-1 mice were infected or mock infected, housed for 30 days, and then killed for tissue as previously described³⁶.

Stem-loop qRT-PCR. Real time quantitative RT-PCR assays were designed for each HSV-1 miRNA and a cellular miRNA, let-7a, with specific stem-loop transcription primers and PCR reagents, as described³⁷. RNA standards, stem-loop RT primers and PCR primers were purchased from IDT, and TaqMan probes were purchased from Applied Biosystems (Supplementary Table 5B). Each assay was performed alongside assays of serial dilutions of each target synthetic standard miRNA, and as a negative control, a pool of all of the other synthetic miRNAs at a concentration corresponding to the lowest dilution of the target miRNA. Furthermore, each assay included reverse transcriptase-negative and reverse transcriptase primer-negative controls. RNA was reverse transcribed in duplicate with Multiscribe (Ambion) and miRNA-specific RT primers. Aliquots of cDNA were assayed on a PRISM 7700 Sequence Detection System (Applied Biosystems). The dynamic range of each assay exceeded five orders of magnitude. To ensure quantification of low levels of mature HSV-1 miRNAs, we first isolated <200-nucleotide-long species (short-enriched) with the mirVana miRNA Isolation Kit (Ambion). RNA was fractionated using a flashPAGE System (Ambion), enriching for <40 nucleotide RNAs. Each <40 nucleotide RNA fraction was assayed for at least seven miRNAs, in duplicate. let-7a was assayed in both the short-enriched and <40 nucleotide RNAs. The number of let-7a molecules per ng of short-enriched RNA was determined (Supplementary Table 5A), and used to normalize the recovery of HSV-1 miRNAs in the <40 nucleotide RNA.

29. Coen, D. M., Fleming, H. E. Jr, Leslie, L. K. & Retondo, M. J. Sensitivity of arabinosyladenine-resistant mutants of herpes simplex virus to other antiviral drugs and mapping of drug hypersensitivity mutations to the DNA polymerase locus. *J. Virol.* **53**, 477–488 (1985).
30. Goldin, A. L., Sandri-Goldin, R. M., Levine, M. & Glorioso, J. C. Cloning of herpes simplex virus type 1 sequences representing the whole genome. *J. Virol.* **38**, 50–58 (1981).
31. Sekulovich, R. E., Leary, K. & Sandri-Goldin, R. M. The herpes simplex virus type 1 α protein ICP27 can act as a *trans*-repressor or a *trans*-activator in combination with ICP4 and ICP0. *J. Virol.* **62**, 4510–4522 (1988).

32. Brummelkamp, T. R., Bernards, R. & Agami, R. A system for stable expression of short interfering RNAs in mammalian cells. *Science* **296**, 550–553 (2002).
33. Wiegand, H. L., Doehle, B. P., Bogerd, H. P. & Cullen, B. R. A second human antiretroviral factor, APOBEC3F, is suppressed by the HIV-1 and HIV-2 Vif proteins. *EMBO J.* **23**, 2451–2458 (2004).
34. Cai, X. *et al.* Kaposi's sarcoma-associated herpesvirus expresses an array of viral microRNAs in latently infected cells. *Proc. Natl Acad. Sci. USA* **102**, 5570–5575 (2005).
35. Alvira, M. R., Goins, W. F., Cohen, J. B. & Glorioso, J. C. Genetic studies exposing the splicing events involved in herpes simplex virus type 1 latency-associated transcript production during lytic and latent infection. *J. Virol.* **73**, 3866–3876 (1999).
36. Leib, D. A. *et al.* Immediate-early regulatory gene mutants define different stages in the establishment and reactivation of herpes simplex virus latency. *J. Virol.* **63**, 759–768 (1989).
37. Chen, C. *et al.* Real-time quantification of microRNAs by stem-loop RT-PCR. *Nucleic Acids Res.* **33**, e179 (2005).